Electronic and optical properties of CeS under pressure

S. K. De and S. Chatterjee
Department of Materials Science, Indian Association for the Cultivation of Science, Calcutta 700 032, India
(Received 30 May 1989)

The electronic band structure of CeS under pressure has been studied by means of self-consistent linear augmented plane-wave method in the local-density approximation. Density of states and partial occupation number are presented as a function of the lattice parameter to assess the variation of valency with pressure. In addition, coefficient of linear specific heat, the imaginary part of the dielectric function, and the real part of optical conductivity are calculated and are compared with the experimental results.

I. INTRODUCTION

The cerium metal and many of its compounds exhibit the isostructural transition under pressure accompanied by a large change of bulk modulus and electronic properties. These effects can be explained by the recent model of the Kondo[1] lattice which includes the increase of mixing interaction between the $4f$ and conduction electrons with decrease of volume. Among these compounds, the cerium monochalcogenides which have NaCl-type structure exhibit metallic conductivities. In these compounds, Ce is present in a trivalent state at normal pressure. Thus, these compounds offer an attractive series for studying the volume behavior as a function of pressure.

Croft and Jayaraman[2] first studied the pressure-volume behavior and also the ambient resistivity versus temperature of CeS. They found that the resistivity shows a Kondo-like behavior between 8 and 30 K. The volume discontinuity of about 4.5% was also observed around 12 GPa with no change in the crystal structure. Recently, Vedel *et al.*[3] studied the pressure-volume relationship for CeS at room temperature up to 25 GPa as shown in the Fig. 1. From this figure it is seen that there is no sharp volume transition—only a smooth variation occurs under pressure. They showed that the disagreement with the previous results is due to the presence of strong anisotropic stresses which were completely neglected by Croft and Jayaraman. The value of bulk modulus they obtained, 83 GPa is in good agreement with other trivalent rare-earth chalcogenides. But the value is slightly smaller than that of LaS.[4] This difference is due to mixing interaction between $4f$ and conduction electrons. As the mixing interaction increases when the volume is reduced, it has a negative contribution to the free energy and therefore gives rise to a reduction of the bulk modulus. Another interesting fact is that the volume of CeS decreases faster than a stable valence compound. At 25 GPa, the additional volume reduction amounts to about 5% which yields a valence increase of about 0.26. Thus, the electronic transition in CeS proceeds at a higher pressure than in CeO (Ref. 5) and at a much reduced rate. Thus a thorough band-structure study of CeS is needed to ascertain these findings.

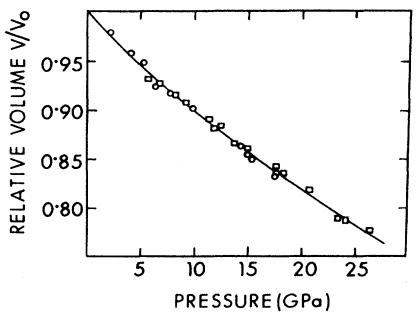

FIG. 1. Relative volume of CeS as a function of pressure.

The self-consistent band-structure calculation as a function of lattice parameter of many cerium compounds has been done to study the electronic properties as a function of pressure. But no such work on CeS has yet been done. Only Soldatov *et al.*[6] studied the non-self-consistent band structure at normal pressure by the Korringa-Kohn-Rostoker (KKR) method. In this work, we have preformed a thorough band-structure calculation by self-consistent linear augmented-plane-wave (LAPW) method of CeS for four lattice constants. We have applied a general form of Hohenberg-Kohn-Sham local-density-functional theory to study the electronic properties of CeS for a range of atomic volumes between normal pressure and 25 GPa. In Sec. II, we describe briefly the methods used. Energy bands and the density of states are discussed in Sec. III. The calculations of specific heat and the optical property are given in Secs. IV and V. The conclusions of this work are summarized in Sec. VI.

II. CALCULATIONAL DETAILS

The band-structure calculations have been carried out using the self-consistent semirelativistic linear augmented-plane-wave method[7–10] in the Hohenberg-Kohn-Sham local-density approximation. The potential is taken in the muffin-tin (MT) form. The parametrization of the local-density approximation of von Barth and Hedin[11] has been used to form the exchange-correlation potential. The lattice constants and the MT radii used in this calculation are given in Table I. The charge density

TABLE I. Input parameters for LAPW calculations, lattice constant a, and muffin-tin radius R_{MT}. E_F is Fermi energy. Distances are in a.u.

a (a.u.)	R_{MT}(Ce) (a.u.)	R_{MT}(S) (a.u.)	E_F (Ry)
$a_1=10.8998$	2.8819	2.5679	0.495
$a_2=10.5236$	2.7889	2.4728	0.580
$a_3=10.3250$	2.7608	2.4017	0.615
$a_4=10.1184$	2.6992	2.3599	0.655

has been calculated by finding out the crystal wave function at 20 **k** points inside the $\frac{1}{48}$ part of the first Brillouin zone.

We have only studied the effect of spin-orbit (s.o.) interaction at Γ and X points. The calculated values of ξ_l^0, ξ_l^1, and ξ_l^2 which give the measure of s.o. interaction[12] are shown in Table II. From Table II it is seen that the maximum splitting occurs for p-like ($l=1$) states of Ce. These states are not important since they are not in the considered energy range. The splitting for p-like states of S is, however, small.

TABLE II. Values of ξ_l^0, ξ_l^1, and ξ_l^2 (mRy).

	l		ξ_l^0	ξ_l^1	ξ_l^2
Ce	1	a_1	66.8	29.9	13.4
		a_4	71.5	26.1	9.5
	2	a_1	5.5	2.2	0.9
		a_4	5.2	1.7	0.5
	3	a_1	3.6	2.7	2.1
		a_4	3.7	2.4	1.6
S	1	a_1	2.5	1.0	0.4
		a_4	2.8	0.9	0.3

III. BAND STRUCTURE AND THE DENSITY OF STATES

The calculated band structures for the four lattice constants corresponding to different pressures along the major symmetry axes in the BZ are shown in Figs. 2–5. Since the s.o. splitting is small in the considered energy range as shown in Table II, we do not show this in the band-structure diagrams. The band structure consists of an occupied sulfur ($3p$) band, unoccupied s and d bands and partially occupied f bands of Ce. The $3p$ (S) band is completely separated from the f bands of Ce. Thus, there is no overlap between the ligand p and metal f bands. The s and d bands of Ce are broad conduction bands. The f bands are therefore immersed in a sea of electrons in s-d conduction bands.

Some important features can be observed from the general behavior of the bands throughout the range of atomic volume. The $3p$ bands of S lie approximately 3 eV below the f bands of Ce. At the X point, X_4' is the lowest point, in contrast to the $2p$ band of oxygen in CeO.[13] Similar to CeN (Ref. 14) and CeO (Ref. 13) due to the strong hybridization between the Δ_1 and Δ_5 bands of the f and $3p$ bands, the Γ_{15} state of the f bands lies above the Γ_{25} state, inverting the f crystal-field levels. Another strong hybridization occurs between the Δ_2' bands derived

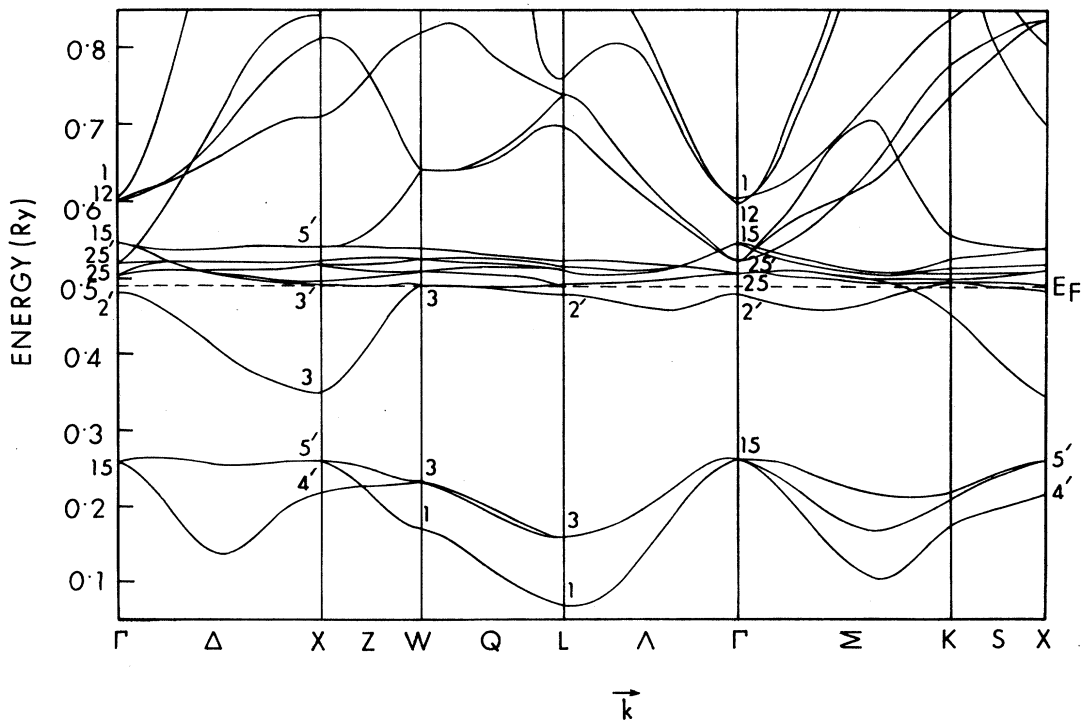

FIG. 2. Band structure along the principal axes for lattice constant a_1. E_F is the Fermi energy.

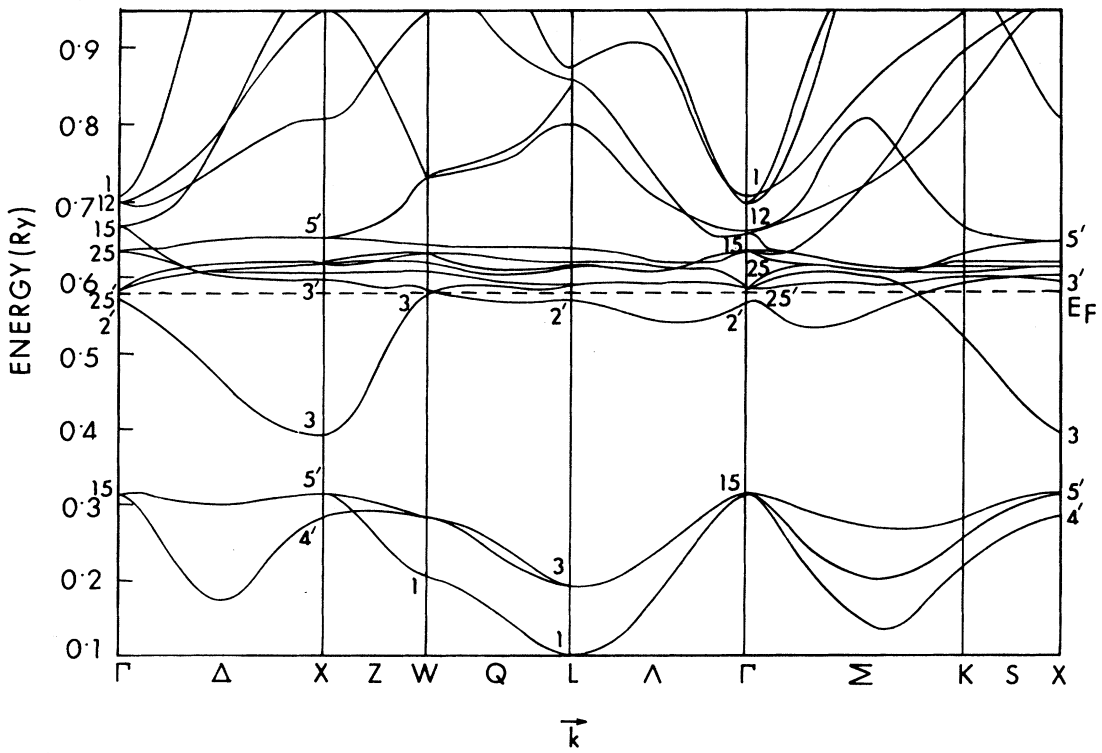

FIG. 3. Band structure along the principal axes for lattice constant a_2. E_F is the Fermi energy.

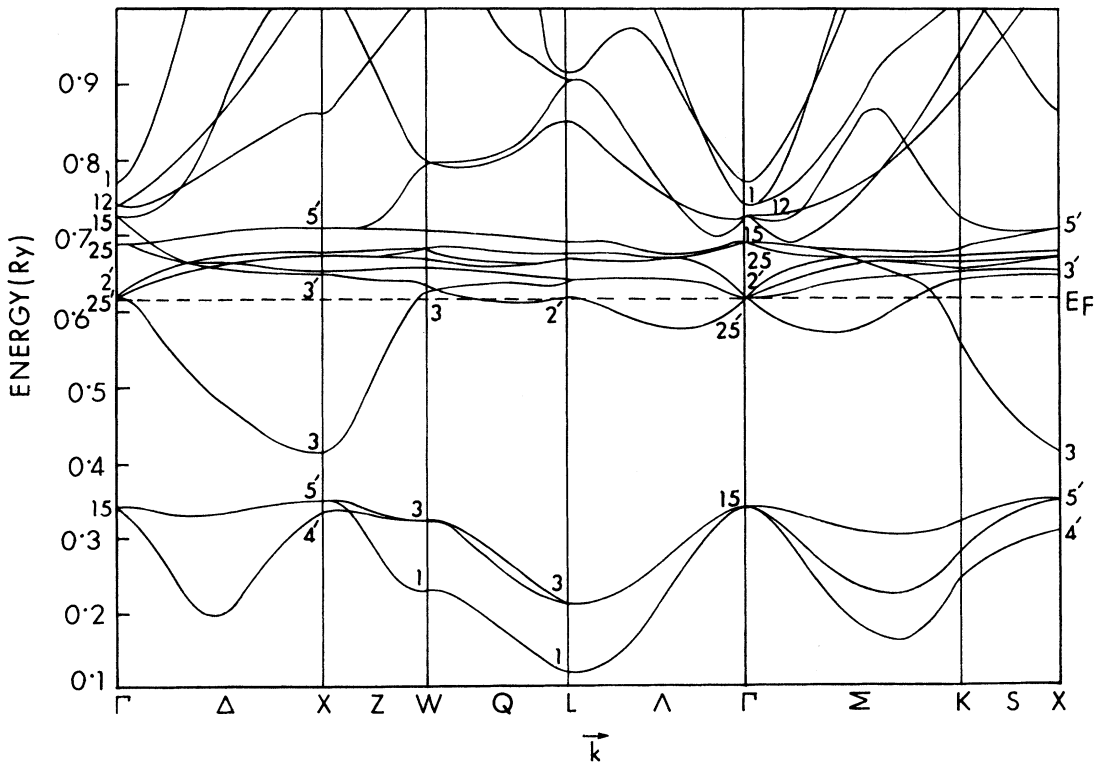

FIG. 4. Band structure along the principal axes for lattice constant a_3. E_F is the Fermi energy.

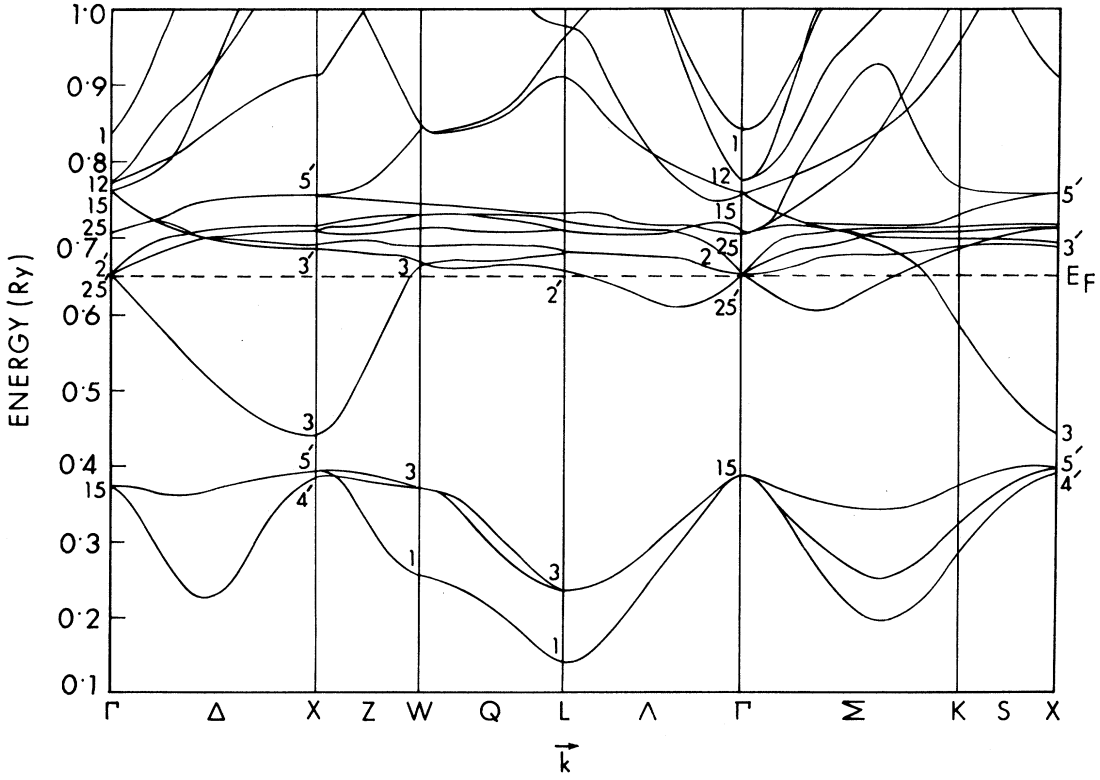

FIG. 5. Band structure along the principal axes for lattice constant a_4. E_F is the Fermi energy.

from the Γ_2' state of the f bands and the Γ_{25}' state of the d bands. As a result of this, the Δ_2' band is completely separated from the f bands of Ce. The f-band width changes from 67 to 107 mRy in going from normal pressure to about 25 GPa. The results of s.o. splitting are shown in Table III at Γ and X points for normal and high pressure. Due to the s.o. splitting the f-band width changes from 67 to 75 mRy for a_1 and 107 to 115 mRy for a_4. Thus, there is about 50% change in f-band width with pressure from normal pressure to 25 GPa.

The partial charge distributions at some symmetry points for a_1 and a_4 in each APW sphere are shown in Table IV. From Table IV it is found that in the lowest three bands, the sulfur $3p$ state is dominant. At the Γ_{15} point of the $3p$ state, the f component is 14%, but at X_5' it is 8%. Thus there occurs p-f mixing along the ΓX direction. We also find that the p and f characters at the lowest Γ_{15} state do not change with pressure. The Γ_2' state is purely f character (90%) which decreases along ΓX and this becomes completely d character (36%) at X_3.

TABLE III. Eigenvalues (mRy) at points Γ and X, showing the effect of including s.o. interaction.

	Γ				X			
	a_1		a_4		a_1		a_4	
	no s.o.	s.o	no s.o.	s.o.	no s.o.	s.o.	no s.o.	s.o.
Γ_{15}	261	256	367	360	221	219	386	376
		266		371	260	255	392	388
						268		407
Γ_2'	478	477	653	652	350	350	438	438
Γ_{25}'	514	510	652	649	490	491	685	683
		516		655	495	492	690	688
Γ_{25}	506	500	705	697	514	507	710	705
		510		710		514		712
					520	526	715	720
Γ_{15}	545	541	760	758	540	539	755	750
		552		767		547		763
Γ_{12}	600	600	775	775	710	710	910	909
Γ_1	605	605	840	840	810	808		

TABLE IV. Valence charge distribution of some selected states.

	States	Energy	Ce sphere	S sphere	Interstitial
a_1	Γ_{15}	0.261	0.14 f	0.70 p	0.14
	Γ_2'	0.478	0.90 f		0.09
	X_4'	0.221	0.11 p	0.62 p	0.26
	X_5'	0.260	0.08 f	0.70 p	0.17
	X_3	0.350	0.36 d		0.54
	X_3'	0.490	0.96 f		0.03
	W_1	0.170	0.08 d	0.62 p	0.23
	W_3	0.230	0.08 p, 0.05 d	0.57 p	0.28
	W_3	0.490	0.14 d, 0.58 f		0.21
	L_1	0.067	0.07 s, 0.07 d	0.50 p	0.37
	L_3	0.162	0.16 d	0.63 p	0.20
	L_2'	0.478	0.85 f		0.14
a_4	Γ_{15}	0.367	0.14 f	0.67 p	0.15
	Γ_{25}'	0.652	0.43 d		0.44
	Γ_2'	0.653	0.85 f		0.14
	X_4'	0.386	0.19 p	0.58 p	0.22
	X_5'	0.392	0.08 p, 0.09 f	0.65 p	0.17
	X_3	0.438	0.32 d	0.1 d	0.57
	W_1	0.255	0.09 d	0.61 d	0.25
	W_3	0.372	0.14 p	0.51 p	0.27
	L_1	0.141	0.07 s, 0.07 d	0.47 p	0.38
	L_3	0.235	0.16 d	0.61 p	0.22

So this Δ_2' band derived from the Γ_2' state hybridizes strongly along the ΓX direction with another Δ_2' band from the Γ_{25}' state. At the Ce site the s component is small.

The behavior of the eigenvalues at Γ and X points under the reduction of volume is shown in the Fig. 6. The Γ_1 s state is more sensitive to volume, moving upwards as the volume is decreased. The states Γ_{12} and Γ_{25}' of the d states do not change appreciably relative to E_F under pressure. The f-band energies increase as the volume decreases, pulling E_F with them and increasing the separation between the valence bands and E_F. From this figure we also observe that the gap between X_3 and X_5' states decreases with an increase of pressure. This is due to the increased hybridization between p-f and f-d bands.

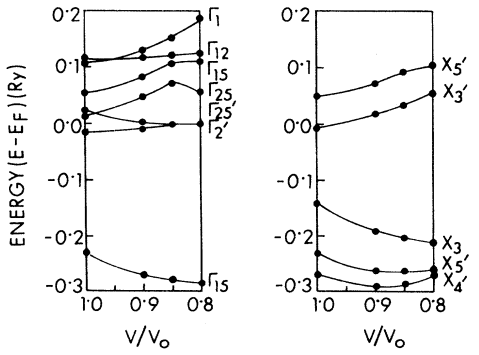

FIG. 6. Behavior of eigenvalues of Γ and X points under reduction of volume. The solid circles represent the calculated results at the four lattice constants.

The density of states (DOS) has been calculated by the tetrahedron method.[15,16] To find the DOS, first-principles eigenvalues are calculated at 89 **k** points. The results of these calculations are shown in Fig. 7. The DOS consists of a huge peak arising from the f bands. The DOS at E_F decreases from 61.957 to 16.532 states/Ry. Throughout the range of atomic volume, the occupied part of the DOS exhibits three peaks. From the partial DOS as shown in Fig. 8, it is seen that the first peak below E_F is due to the f state of Ce and the second and third peaks are due to the $3p$ states of sulfur. At normal pressure, Croft *et al.*[17] studied the occupied DOS by the photoemission experiments. They obtained the two peaks below E_F around 0.66 and 2.5 eV due to the d and f states of Ce. These two peaks correspond to our peaks around 0.2 eV above E_F and around 0.1 eV below E_F. They obtained another two peaks around 5 and 7 eV below E_F which are around 4 and 5 eV in our theoretical calculation. The bottom of the $3p$ band of S lies about 6 eV and the top about 3 eV below E_F. The positions of the peaks derived from the $3p$ state of S move away from E_F with an increase of pressure and also the height of these two peaks decreases with an increase of pressure. The peaks above E_F are mainly derived from the d state of Ce as observed from the partial DOS shown in Fig. 8.

The angular momentum decomposed DOS at E_F and the corresponding charges inside the spheres are shown in Table V. The $6s$ electrons are mainly distributed between the MT spheres. The $3p$ electrons of S decrease from 3.677 to 3.516 with an increase of pressure. The number of f electrons decreases from 1.026 to 0.701 with an increase of pressure. While the d electrons increase

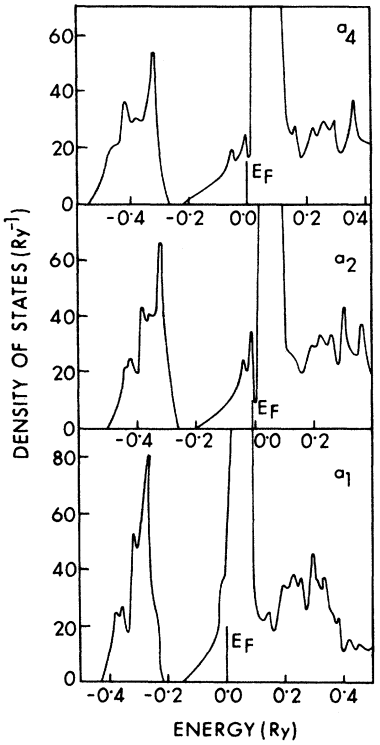

FIG. 7. Density of states at the lattice constants a_1, a_2, and a_4 as a function of energy.

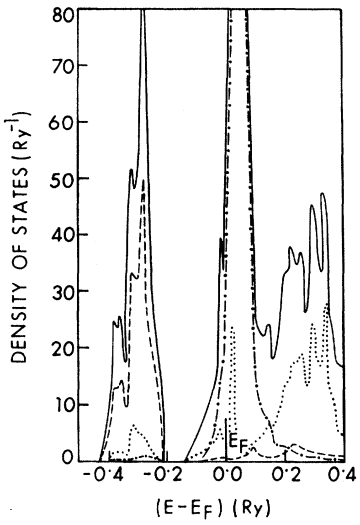

FIG. 8. Total density of states (——) and partial density of states for d (. . . .) and f (—·—·—·) components of Ce and the p (— — —) component of S.

from 0.817 to 0.847 in going from normal pressure to about 25 GPa. Thus, the f electrons are being transferred to d electrons and consequently the valency of Ce in CeS increases with pressure. We also observe from Fig. 6 that the f band rises in energy relative to the conduction d band, which indicates that there occurs f- to d-electron transfer.

IV. SPECIFIC HEAT

We have calculated the linear contribution to the specific heat (γ) at normal and high pressure. The value of γ is given by

$$\gamma=\pi^2 k_B^2(1+\lambda)N(E_F)/3\ , \tag{1}$$

where k_B and λ are Boltzmann's constant and the electron-phonon coupling constant, respectively. λ is given in terms of Ce and S sites by[18]

$$\lambda=\eta_{Ce}/(M_{Ce}\langle\omega^2\rangle_{Ce})+\eta_S/(M_S\langle\omega^2\rangle_S)\ , \tag{2}$$

where M_α and $\langle\omega^2\rangle_\alpha$ are the atomic mass and the mean-squared phonon frequency for atom α. Due to this separation the heavy Ce atom vibrates mainly in the acoustic range of frequencies, the light S atom in the optical range. Neglecting the contribution of electron–optical-phonon interaction to λ we have

$$\lambda\simeq\eta_{Ce}/(M_{Ce}\langle\omega^2\rangle_{Ce})\ . \tag{3}$$

The electron-ion interaction constant η_α has been calculated using the rigid-muffin-tin approximation of Gaspari and Gyorffy,[19]

TABLE V. Angular momentum decomposed muffin-tin density of states at E_F, $N_l(E_F)$, and corresponding charges Q_l.

		Ce					S				
		s	p	d	f	g	s	p	d	Interstitial	Total
$N_l(E_F)$	a_1	0.005	0.112	1.592	52.540	0.025	0.418	0.786	0.085	6.394	61.957
(states/Ry)	a_2	0.004	0.199	0.871	11.943	0.010	0.003	0.124	0.514	3.864	17.532
	a_3	0.006	0.192	2.068	9.235	0.016	0.003	0.178	0.771	4.739	17.208
	a_4	0.005	0.188	1.960	8.787	0.017	0.003	0.177	0.785	4.610	16.532
Q_l	a_1	0.089	0.176	0.817	1.026	0.009	0.011	3.677	0.102	2.093	8.000
	a_2	0.084	0.249	0.833	0.752	0.010	0.013	3.653	0.131	2.275	8.000
	a_3	0.085	0.293	0.863	0.696	0.011	0.015	3.564	0.137	2.336	8.000
	a_4	0.083	0.331	0.847	0.701	0.011	0.018	3.516	0.146	2.347	8.000

$$\eta_\alpha = \frac{E_F}{\pi^2 N(E_F)} \sum_l 2(l+1)\sin^2(\delta_{l+1}^\alpha - \delta_l^\alpha) \times \frac{N_l^\alpha N_{l+1}^\alpha}{N_l^{(1)\alpha} N_{l+1}^{(1)\alpha}} . \quad (4)$$

In this expression δ_l^α are the scattering phase shifts at E_F for atom α and angular momentum l and $N_l^{(1)\alpha}$ are the single-scatter densities of states for atom α and angular momentum l at E_F.

To calculate λ we need $\langle\omega^2\rangle$. Butler[20] has found the relation $\langle\omega^2\rangle^{1/2} = 0.69\Theta_D$, Θ_D being the Debye temperature. Since there is no experimental value of Θ_D, we have calculated Θ_D from the relation[21]

$$\Theta_D = [\hbar V/(k_B R_e)]\{-\tfrac{5}{2}(1/M_{\mathrm{Ce}} + 1/M_{\mathrm{S}}) \times [P' + 4P/(3V)]\}^{1/2} , \quad (5)$$

where R_e is intra-atomic distance at volume V and P' is the first derivative of P with respect to V. P' has been calculated from the experimental value of the bulk modulus.[3] The calculated values of Θ_D are 395.7 and 305.8 K at normal pressure and at about 25 GPa.

The values of δ_l^α and the contribution to η up to the transitions with $l = 3 \leftrightarrow 4$ for the Ce atom and $l = 1 \leftrightarrow 3$ for the S atom are shown in Table VI. The main contribution to η_{Ce} comes from $p \leftrightarrow d$ and $f \leftrightarrow g$ transitions in the Ce atom both at normal (high) pressure. The calculated values of λ and γ are 0.030 (0.051) and 11.44 (3.56) mJ/mol K^2 at normal (high) pressure. At normal pressure γ is large compared to high pressure due to the large density of states. Since there is no experimental value of γ, we are unable to compare with the experiment. But the value of γ at high pressure is nearer to the value (3.07) for CeO.[13]

TABLE VI. Phase shifts δ_l and contribution $\eta_{l,l+1}$ to η (eV Å^{-2}).

		l	δ_l	$\eta_{l,l+1}$	η
a_1	Ce	0	−1.115		
		1	−0.561	0.027	
		2	0.632	0.100	0.563
		3	−0.193	0.436	
		4	0.0003		
	S	0	1.540		
		1	−1.150	0.122	0.154
		2	0.076	0.032	
a_4	Ce	0	−1.404	0.003	
		1	−0.775	0.251	
		2	0.594	0.002	0.565
		3	0.852	0.309	
		4	0.0005		
	S	0	1.333		
		1	−1.288	0.251	
		2	0.125	0.226	0.491
		3	0.003	0.014	

V. OPTICAL PROPERTY

The optical properties of materials are contained in the imaginary part of the dielectric function,

$$\epsilon_2(\omega) = \frac{e^2}{\pi m^2 \omega^2} \sum_{\substack{n_i(\mathrm{occupied}) \\ n_f}} \int_{\mathrm{BZ}} |P_{fi}|^2 \delta(E_{n_f}(\mathbf{k}) - E_{n_i}(\mathbf{k}) - \hbar\omega) d^3k , \quad (6)$$

where $\hbar\omega$ is the energy of incident light and P_{fi} is the optical matrix element. The k-space integral over the δ function yields the joint density of states (JDOS) $\mathcal{N}$. Thus, if the matrix elements P_{fi} are assumed to be constant throughout the Brillouin zone, then

$$\epsilon_2(\omega) \propto \mathcal{N}/\omega^2 . \quad (7)$$

The approximation of constant matrix elements, which we have used in this work, only affects the strength of the peaks, but has little or no effect on the position of structures.[22] We have calculated the JDOS by the Lehman-Taut tetrahedron method,[16] as we did for the DOS calculation.

The peaks and structures observed in $\epsilon_2(\omega)$ spectra as shown in Fig. 9 can be explained in terms of interband transitions. The peak around 2 eV is due to the transition around Γ_2' to around Γ_{12}. The small structure around 2.5 eV arises due to the transition around X_3 to f bands. The large peak around 4.5 eV originates due to transition from the second band along the Δ axis, the second and third bands along the Z axis, the second band along the Λ axis, and the third band along the Σ axis to f bands. The small structures around 7 and 8 eV are due to the transitions around W_3, L_3 and W_1, L_1. From Fig. 9 we observe that the positions of the peaks move towards higher energy with the increase of pressure. The height of the peaks, however, decreases with an increase of pres-

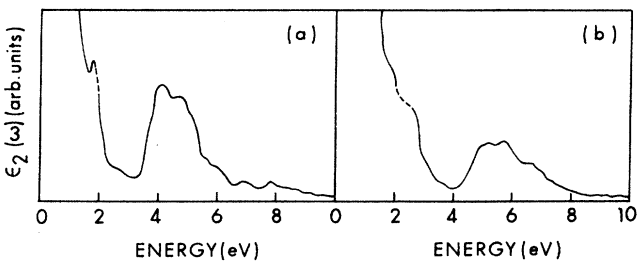

FIG. 9. $\epsilon_2(\omega)$ spectra at two lattice constants (a) a_1 and (b) a_4.

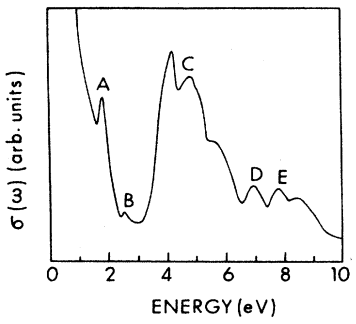

FIG. 10. $\sigma(\omega)$ spectra for lattice constant a_1.

sure. As a result, we do not observe the small peaks around 7 and 8 eV at high pressure.

We have also studied the real part of the optical conductivity $\sigma(\omega)$ from the following relation:

$$\sigma(\omega) \propto \omega \epsilon_2(\omega) \ . \tag{8}$$

The calculated $\sigma(\omega)$ at normal pressure is shown in Fig. 10 at normal pressure. Schoenes[23] experimentally studied the optical conductivity of CeS at normal pressure. The main features of the experimental results may be summarized as follows: two very weak structures near 2.5 and 4.5 eV and the two peaks near 6.5 and 8 eV. These features can be compared with our theoretical results which show a peak near 2 eV (A), a small structure around 2.5 eV (B), a peak around 4.5 eV (C), and two small peaks around 7 eV (D) and 8 eV (E). Thus, the energetic positions of the peaks and structures show fairly good agreement with the experimental results. The energy change of $\sigma(\omega)$ can be understood from the partial DOS shown in Fig. 8. Peak A is due to mainly $4f \rightarrow 5d$ transition, peak B to $5d \rightarrow 4f$, and C to $(3p5d) \rightarrow 4f$ transitions. Peaks D and E are due to the major $3p \rightarrow 5d$ transitions.

VI. CONCLUSION

Vedel *et al.*[3] experimentally found a smooth variation of volume and a continuous valence transition in CeS between normal pressure and 25 GPa. From our band-structure calculations we find that the transfer of electrons from the f to the conduction d band occurs. This shows that a valence transition in CeS occurs under pressure. We also find from our band-structure calculations that the f-band width increases by 50% between normal pressure and 25 GPa. Thus, under reduction of volume, the f shell of Ce in CeS is delocalized. As there is no discontinuous change in volume, so there is no abrupt change in the f-band width. The Ce-Ce distance in CeS is 4.08 Å, which is higher than the critical value 3.40 Å for the occurrence of γ-α transitions.[24] Thus there may be a transition like γ-α in CeS at much higher pressure.

The calculated results are compared with the experiments. The energy positions of the peaks and structures of $\sigma(\omega)$ spectra are in excellent agreement with the experimental results of Schoenes[23] at normal pressure. As such experiments are not available at higher pressure, we could not compare our results with the experiments. Thus, experiments at higher pressure are needed to find the possibility of electronic transition in CeS.

[1]M. Lavagna, C. Lacroix, and M. Cyrot, Phys. Lett. **90A**, 210 (1982).
[2]M. Croft and A. Jayaraman, Solid State Commun. **35**, 203 (1980).
[3]I. Vedel, A. M. Redon, J. M. Leger, J. Rossat-Mignod, and O. Vogt, J. Phys. C **19**, 6297 (1986).
[4]A. Jayaraman, B. Batlogg, R. G. Maines, and H. Bach, Phys. Rev. B **26**, 3347 (1982).
[5]I. Vedel, A. M. Redon, and J. M. Leger, J. Phys. C **19**, 3549 (1986).
[6]A. V. Soldatov, Gusatinskil, and Alperovich, Fiz. Tverd. Tela (Leningrad) **27**, 3423 (1985) [Sov. Phys.—Solid State **27**, 2061 (1985)].
[7]D. D. Koelling and G. O. Arbman, J. Phys. F **5**, 2041 (1975).
[8]D. D. Koelling and B. N. Harmon, J. Phys. C **10**, 3107 (1977).
[9]W. E. Pickett, A. J. Freeman, and D. D. Koelling, Phys. Rev. B **23**, 1266 (1981).
[10]S. K. De and S. Chatterjee, J. Phys. F **17**, 2057 (1987).
[11]U. von Barth and L. J. Hedin, J. Phys. C **5**, 1629 (1972).
[12]A. H. MacDonald, W. E. Pickett, and D. D. Koelling, J. Phys. C **13**, 2675 (1980).
[13]S. K. De and S. Chatterjee, J. Phys. Condens. Matter **1**, 1169 (1989).
[14]S. K. De and S. Chatterjee, J. Phys. C **21**, 3261 (1988).
[15]O. Jepsen and O. K. Andersen, Solid State Commun. **9**, 1763 (1971).
[16]G. Lehman and M. Taut, Phys. Status Solidi B **54**, 469 (1972).
[17]M. Croft, A. Franciosi, J. H. Weaver, and A. Jayaraman, Phys. Rev. B **24**, 544 (1981).
[18]B. M. Klein and D. A. Papaconstantopoulos, J. Phys. F **6**, 1135 (1976).
[19]G. P. Gaspari and B. L. Gyorffy, Phys. Rev. Lett. **28**, 801 (1972)
[20]W. H. Butler, Phys. Rev. B **15**, 5267 (1977).
[21]J. Hama and M. Watanabe, Phys. Lett. **115A**, 287 (1986).
[22]W. E. Pickett and P. B. Allen, Phys. Rev. B **11**, 3593 (1975).
[23]J. Schoenes, *Moment Formation in Solids,* edited by W. J. L. Buyers (Plenum, New York, 1984), p. 237.
[24]W. E. Pickett and B. M. Klein, J. Less-Common Met. **93**, 219 (1983).